Fibers and Polymers 2013, Vol.14, No.5, 793-803 DOI 10.1007/s12221-013-0793-0

Miscibility and Performance Evaluation of Natural-Flour-Filled PP/PBS and PP/PLA Bio-Composites

Hee-Soo Kim[1,2] and Hyun-Joong Kim[2,3]*

[1]*Advanced Meterials Research Institute, Biomaterial Technology Part, Samsung Fine Chemicals Co., Ltd., Daejun 305-380, Korea*
[2]*Laboratory of Adhesion & Bio-Composites, Program in Environmental Materials Science, Seoul 151-921, Korea*
[3]*Research Institute for Agriculture and Life Sciences, Seoul National University, Seoul 151-921, Korea*
(Received September 3, 2011; Revised September 5, 2011; Accepted October 10, 2011)

Abstract: This research evaluates the miscibility and performance of polypropylene (PP)/polybutylene succinate (PBS) and PP/polylactic acid (PLA) blend and natural-flour-filled, PP/PLA and PP/PBS blend bio-composites. The melting temperature (T_m) and glass transition temperature (T_g) of pure PP, PBS and PLA showed a single peak but differential scanning calorimetry (DSC) and dynamic mechanical thermal analysis (DMTA) presented two peaks for the T_m and T_g of the PP/PBS and PP/PLA blends. These results indicated that the PP/PBS and PP/PLA blend systems existed as immiscible blends. These results were also confirmed by the scanning electron microscopy (SEM) micrographs of the tensile fracture surface of the PP/PBS and PP/PLA blends. At a PP/PBS and PP/PLA blend ratio of 70/30, the tensile and flexural strengths of bamboo flour (BF)- and wood flour (WF)-filled, PP/PBS and PP/PLA blend bio-composites were similar to those of BF- and WF-filled, PP and PBS bio-composites. In addition, these strengths of maleic anhydride-grafted PP (MAPP)- and acrylic acid-grafted PP (AAPP)-treated, BF- and WF-filled, PP/PBS and PP/PLA blend bio-composites were higher than those of non-treated bio-composites.

Keywords: Natural flour, Bio-composites, Miscibility, Interfacial adhesion, Mechanical properties

Introduction

In recent years, the extensive use of non-biodegradable plastics has led to serious environmental pollution due to their non-biodegradability [1,2]. The use of biodegradable plastics and bio-composites instead of conventional non-biodegradable plastics is one of the ultimate available solutions to the environmental problems caused by the disposal of biostable plastic wastes [3]. Bio-composites composed of biodegradable polymer as matrix polymer and bio-fillers (natural fiber and flour) as reinforcing fillers have attracted research attention due to their capability to protect the natural environment [2,4]. Natural fillers have advantages such as wide availability, high specific strength and modulus, low density, low cost, low CO_2 emission, ease of surface modification, relative non-abrasiveness and biodegradability [5].

Biodegradable plastics have recently attracted much attention because they can replace the non-biodegradability plastics that cause environment problems. However, biodegradable plastics generally present some problems because of their high price and the limited variety of biodegradable plastics that are commercially available. So far, the high price of these bio-degradable polymers in comparison to conventional plastics has limited their general application. To solve these problems, polymer blending and copolymerization techniques have been tried by many researchers to obtain biodegradable polymers [3]. A trend has also developed towards the production of mixtures of biodegradable polymers and conventional polymers due to the continuing high cost of producing biodegradable materials [6,7]. Polymer blends may open a new window for product diversity and materials that can overcome the property requirements for a specific application. Blending these two kinds of polymer together is of significant interest, since it could lead to the development of a new range of biodegradable polymeric materials [8,9].

Therefore, we investigated the use of natural-flour-filled, biodegradable polymer and polypropylene (PP) as conventional, non-biodegradable polymer, blend bio-composites in order to improve the mechanical and thermal properties and reduce the production costs. In this study, the matrix polymers polylactic acid (PLA) and polybutylene succinate (PBS) were used as biodegradable polymers and the natural flours wood flour (WF) and bamboo flour (BF) were used as reinforcing fillers. PP is a widely used matrix polymer in natural-filler reinforced composites because of its excellent mechanical and thermal properties, light weight, chemical resistance, low cost, ease of processing and good recycling properties [10]. PLA and PBS are biodegradable, aliphatic, thermoplastic polymers that can be produced from renewable resources. PLA is a highly versatile, biodegradable aliphatic polyester derived from 100 % renewable resources, such as corn and sugar beet. PLA is synthesized by the ring-opening polymerization of lactides, which are the cyclic dimmers of lactic acids and are typically derived from corn starch fermentation [11,12]. PBS is chemically synthesized by the polycondensation of 1,4-butanediol and succinic acid and is commercially available with many desirable properties including biodegradability, melt processibility and excellent thermal and chemical resistance. The 1,4-butanediol and succinic acid, which are the raw materials for PBS, can be produced by using bio-based renewable resources from starch fermentation [13,14]. BF and WF have found wide use as completely biodegradable, biomass materials and natural

*Corresponding author: hjokim@snu.ac.kr

fillers. Especially, BF is an abundant natural resource in Asia, and it can be renewed much more rapidly than WF due to bamboo's more rapid growth than wood. Because of this property, BF has gradually invaded wood forests and reduced the wood supply [15]. Because BF has limited industrial application, the use of BF as a reinforcing filler for bio-composites materials will provide many benefits. For enhancement of the interfacial adhesion between matrix polymer and natural flour of bio-composites was used as a compatibilizer.

The aim of the current research was to evaluate the miscibility, manufacture and performance of PP/PLA and PP/PBS blends and natural-flour-filled, PP/PLA and PP/PBS bio-composites. We measured the mechanical properties and miscibility in the PP/PLA and PP/PBS blends using differential scanning calorimetry (DSC), dynamic mechanical analysis (DMA) and thermogravimetric analysis (TGA). The interaction between the PP/PBS and PP/PLA blend phases was examined with scanning electron microscopy (SEM). In addition, the mechanical properties of the bio-composites were investigated and morphological observations were made.

Experimental

Materials

Matrix Polymer and Natural Flour

PP was supplied by LG Chemical Co., South Korea, with an MFI of 12 g/10 min and a density of 0.9 g/cm^3. PBS was prepared at Ire Chemical Ltd., South Korea, with an MFI of 25 g/10 min and a density of 1.26 g/cm^3. PLA was supplied by Cargill-Dow Co. USA with an MFI of 15 g/10 min (190 ^{o}C/2, 160 g) and a density of 1.22 g/cm^3. The natural flours used as the reinforcing filler, BF and WF, were supplied by Hangyang Advanced Materials Co. South Korea. The particle size of BF and WF was 860 to 270 μm, and 140 μm, respectively.

Maleic anhydride-grafted PP (MAPP) was obtained from Eastman Chemical Products, Inc., in the form of Epolene G-3003, which has an acid number of 8 and a molecular weight of 52,300. Acrylic acid-grafted PP (AAPP) was obtained from Crompton Co., in the form of Polybond 1002, which has an acrylic acid content of 8.

Compounding and Sample Preparation

BF and WF were oven dried at 105 ^{o}C for 24 hrs to adjust the moisture content to 1~3 % and then stored in sealed polyethylene bags before compounding. PP/PLA and PP/PBS were blended with the BF and WF in a laboratory-sized, co-rotating, twin screw extruder using three general processes: melt blending, extrusion and pelletizing. The extruder barrel was divided into eight zones with the temperature in each zone being individually adjustable. Table 1 shows the blending ratio of PP/PLA and PP/PBS blend biocomposites. Also, to enhance interfacial adhesion, the 30 wt.% filler loading was prepared by incorporating 5 % MAPP and AAPP. The temperature of the mixing zone in the barrel was maintained at 185 ^{o}C with a screw speed of 250 rpm. The extruded strand was cooled in a water bath and pelletized using a pelletizer. The extruded pellets were oven dried at 80 ^{o}C for 24 hrs and stored in sealed polyethylene bags to avoid unexpected moisture infiltration. Extruded pellets were injection molded into tensile (ASTM D638) and three-point bend test bars (ASTM D790) using an injection molding machine (Bau Technology, South Korea) at 190 ^{o}C with an injection pressure of 1,200 psi and a device pressure of 1,500 psi. After injection molding, the test bars were conditioned before testing at 50 ± 5 % RH for at least 40 hours according to ASTM D 618-99.

Table 1. Blending ratio of PP/PLA, PP/PBS, natural flour and compatibilizing agents

	Blend ratio of PP/PLA and PP/PBS				
PLA, PBS	10	30	50	70	10
PP	90	70	50	30	90
Natural flour (BF, WF)	30 wt.%				
Compatibilizing agents	5 wt.%				

Miscibility Measurement

Mechanical Property

The tensile test for the PP/PLA and PP/PBS blends was conducted according to ASTM D 638-99 with a Universal Testing Machine (Zwick Co.) at a crosshead speed of 5 mm/min and a temperature of 24±2 ^{o}C. Five measurements were conducted and averaged for the final result.

Thermogravimetric Analysis (TGA)

TGA measurements of the PP/PLA and PP/PBS blends were carried out using a thermogravimetric analyzer (TGA Q500, TA instruments) on samples of about 10~13 mg, over a temperature range from 25 ^{o}C to 700 ^{o}C, at a heating rate of 20 ^{o}C/min, under a nitrogen flow of 40 ml/min. TGA was measured with the bio-composites placed in a high quality nitrogen (99.5 % nitrogen, 0.5 % oxygen content) atmosphere to prevent unwanted oxidation.

Differential Scanning Calorimetry (DSC)

DSC analysis was carried out using a TA Instrument DSC Q 1000 with 3~5 mg of PP/PLA and PP/PBS blends at the designated time points. Each sample was scanned as the dynamic mode was raised from −80 to 200 ^{o}C at a heating rate of 10 ^{o}C/min and then cooled at the same rate under a nitrogen atmosphere. Glass transition (T_g), melting (T_m) and crystallization (T_c) temperatures were determined from the second scan. T_m was taken as the maximum of the endothermic melting peak, T_c as the temperature at the top of the crystallization peak, and T_g as the deflection of the baseline from the cooling scan. The heats of fusion (ΔH_f) and crystallization (ΔH_c) were determined from the areas of the melting and crystallization peaks, respectively.

Dynamic Mechanical Analysis (DMA)

The viscoelastic properties of the PP/PLA and PP/PBS blends were measured using a dynamic mechanical analyzer

(DMA Q500, TA instruments). Rectangular specimens of dimensions 35.0 mm×12.0 mm×3.0 mm were used using the dual cantilever method. The measurements were performed at a frequency of 1 Hz and at a strain rate 0.1 %. The temperature range was from −80 to 100 °C at a scanning rate of 2 °C/min. The storage modulus (E'), loss modulus (E'') and loss factor (tan δ) of the specimens were measured as a function of temperature.

Morphological Observation

SEM was used to observe the PP/PLA and PP/PBS blends using a SIRIOM scanning electron microscope (FEI Co.) from the USA. Prior to the measurement, the specimens were coated with gold (purity, 99.99 %) to eliminate electron charging.

Bio-Composites Measurement

Mechanical Properties

The tensile test for the bio-composites was conducted according to ASTM D 638-99 with a Universal Testing Machine (Zwick Co.) at a crosshead speed of 5 mm/min and a temperature of 24±2 °C. The three-point bend tests of the bio-composites were carried out in accordance with ASTM D 790. The specimens had a span to depth ratio of 16:1 with a crosshead speed of 5 mm/min. Five measurements were conducted and averaged for the final result.

Attenuated Total Reflectance (FTIR-ATR) Spectroscopy

The infrared spectra in the bio-composites were obtained using a JASCO 6100 FTIR-ATR spectrophotometer from Japan. The specimens were analyzed over the range of 4000~600 cm^{-1} with a spectrum resolution of 4 cm^{-1}. All spectra were averaged over 32 scans. This analysis was performed at a point-to-point contact with a pressure device when analyzing the bio-composites.

Morphological Observation

SEM was used to measure the bio-composites the using a SIRIOM scanning electron microscope (FEI Co.) from the USA. Prior to the measurement, the specimens were coated with gold (purity, 99.99 %) to eliminate electron charging.

Results and Discussion

Miscibility Measurement

Mechanical Property

The tensile strength and modulus of the PP/PBS and PP/PBS blends is shown in Figure 1. The tensile strength of the PP/PBS blends decreased with increasing PBS content, indicating the incompatibility of the PP/PBS blends. However, the tensile modulus of the PP/PBS blends did not significant change. PBS is a biodegradable aliphatic polyester, and the presence of the ester groups of the PBS main chain will reduce the tensile strength of the PP/PBS blend. This incompatibility between PP and PBS is responsible for the very poor mechanical properties due to poor stress transfer across the interface [16]. However, the tensile strength and modulus of the PP/PLA blends increased with increasing PLA content, indicating the higher tensile strength and modulus of PLA compared to PP. Therefore, we expected the natural-flour-filled, PP/PLA blend bio-composites to exert a greater effect than that of the PP/PBS blend bio-composites due to the higher tensile strength of the PP/PLA blends. Figure 2 shows the tensile load (N) versus elongation (%) curves of the (a) PP/PBS and (b) PP/PLA blends. The pure PLA showed very brittle behavior, unlike the pure PBS which behaved as a ductile material. With increasing PBS content, the tensile load and elongation of the PP/PBS blends decreased due to the low compatibility of two polymers. However, the PLA content in the PP reduced their ductility and increased their brittleness under tensile deformation.

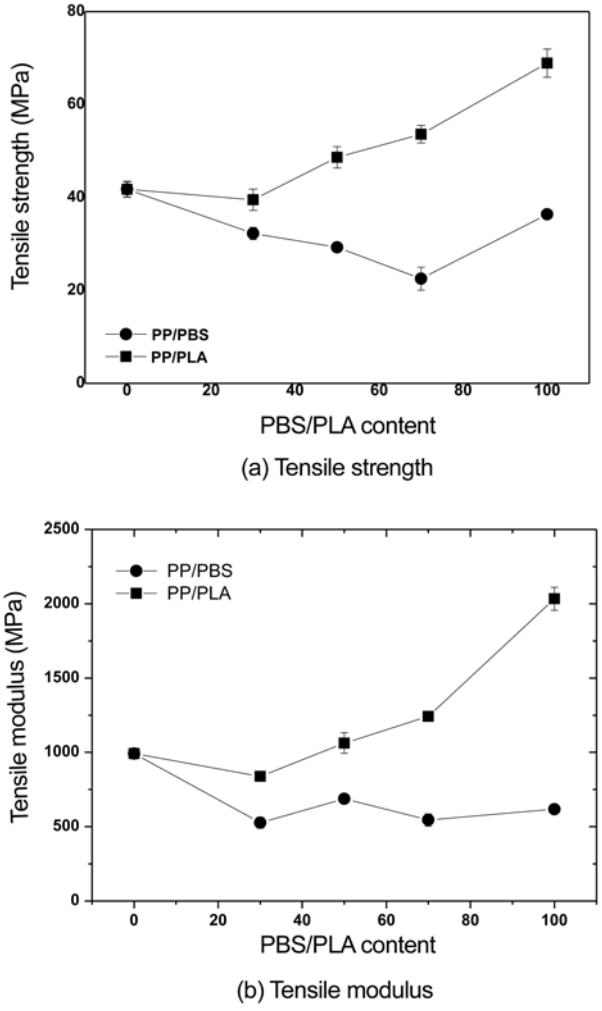

Figure 1. Tensile strength (a) and tensile modulus (b) of PP/PBS and PP/PLA blends as a function of composition.

Thermogravimetric Analysis (TGA)

The TGA curves of the (a) PP/PBS and (b) PP/PLA blends are shown in Figure 3. PP and PBS apparently suffered a dramatic decrement of heat within the designated temperature range at 477.3 °C and 423.3 °C, respectively. These results were confirmed by the DTG_{max} degradation temperature results

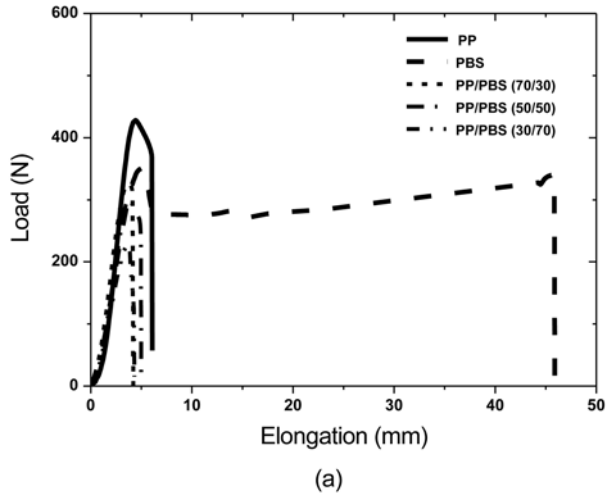

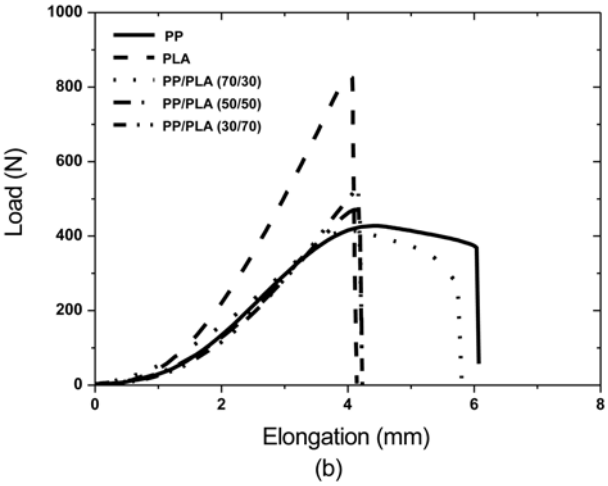

Figure 2. Tensile load (N) versus elongation curves of (a) PP/PBS and (b) PP/PLA blends.

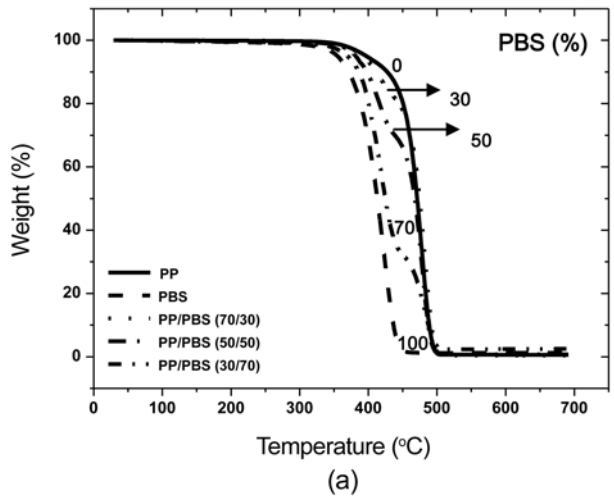

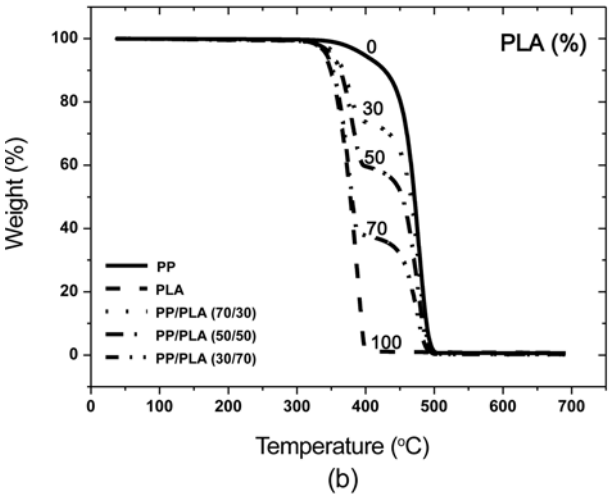

Figure 3. TGA curves of (a) PP/PBS and (b) PP/PLA blends as a function of composition.

shown in Figure 4. This result suggested that PP and PBS were composed of a series of interchained monomers. In this case, increasing temperature would promote the decreasing molecular weight and the increasing chain scission to occur at the weak sites of the polymer chains, which would then induce the formation of oligomers or monomers. These oligomers or monomers would break down further into gases due to the temperature increase [17]. In Figures 3 and 4, the thermal stability and degradation temperature of PP were higher than those of PBS and PLA, possibly because the ester bonds in the PBS and PLA main-chain were more easily decomposed at a lower temperature than that of the carbon-carbon bonds in the PP main-chain. This result indicated that the thermal stability of biodegradable polymers such as PBS and PLA is lower than that of non-biodegradable polymers such as PP.

The main difference between the degradation of pure homopolymers and that of polymer blends arises from the interactions that may occur between different species in the blends during

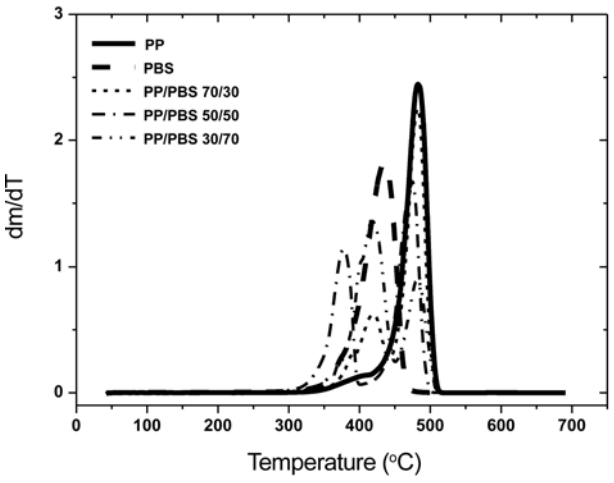

Figure 4. DTG_{max} degradation temperature of PP/PBS and PP/PLA blends as a function of composition.

Table 2. DTG_{max} temperature of PP/PBS and PP/PLA blends as a function of composition

Sample	Peak 1	Peak 2
PP	477.3	-
PBS	423.3	-
PP/PBS (70/30)	419.9	480.2
PP/PBS (50/50)	382.6	478.4
PP/PBS (30/70)	418.1	483.5
PLA	391.5	-
PP/PLA (70/30)	381.7	479.1
PP/PLA (50/50)	382.1	478.9
PP/PLA (30/70)	379.5	477.6

degradation and among the products of degradation [18]. With increasing PBS content, the thermal degradation region of the binary PP/PBS blends clearly exhibits two mass loss steps: the first between 400 and 450 °C due to the thermal degradation of PBS, and the second approximately between 400 and 450 °C due to the thermal degradation of PP. These results were also seen in Figure 3(b), and were clearly confirmed by the DTG_{max} temperatures of the PP/PBS and PP/PLA blends (Table 2). The thermal stability and degradation temperature of the PP/PBS and PP/PLA blends decreased with increasing PBS and PLA content. These results were attributed to the lower thermal stability of PBS and PLA. In addition, the thermal degradation region of the PP/PBS and PP/PLA blends clearly showed the mass loss steps, as demonstrated by the poor compatibility and immiscibility of the PP/PBS and PP/PLA blends between the two phases.

Differential Scanning Calorimetry (DSC)

DSC is a useful indirect method to analyze polymer blends. DSC is used to quantitatively measure phenomena associated with both thermodynamic and kinetic process such as crystallization, T_m, T_g, curing reaction, and aging of polymer and their blends (George, 2003). In order to examine the miscibility of the PP/PBS and PP/PLA blends, this study measured T_g and T_m of these blends using DSC. Polymer blends can be generally divided into two main groups: compatible or incompatible and miscible or immiscible (George, 2003). Figure 5 shows the DSC second thermograms of the (a) binary PP/PBS and (b) PP/PLA blends. The T_m of pure PP, PBS and PLA showed a single peak at 167.8, 114.0, and 151.3 °C, respectively. However, two well-separated melting peaks were found for the PP/PBS and PP/PLA blends, confirming their incomplete miscibility (John *et al*., 2002). The DSC test results of the PP/PBS and PP/PLA blends from the cooling and heating thermogram are listed in Table 3-3. Also, pure PP, PBS and PLA exhibited a single T_g peak whereas the PP/PBS and PP/PLA blends exhibited two T_g peaks. The miscibility between any two polymers in the amorphous region is evidenced by the presence of a single T_g in polymer blend systems [18,19]. These results indicated that the PP/PBS and PP/PLA blend

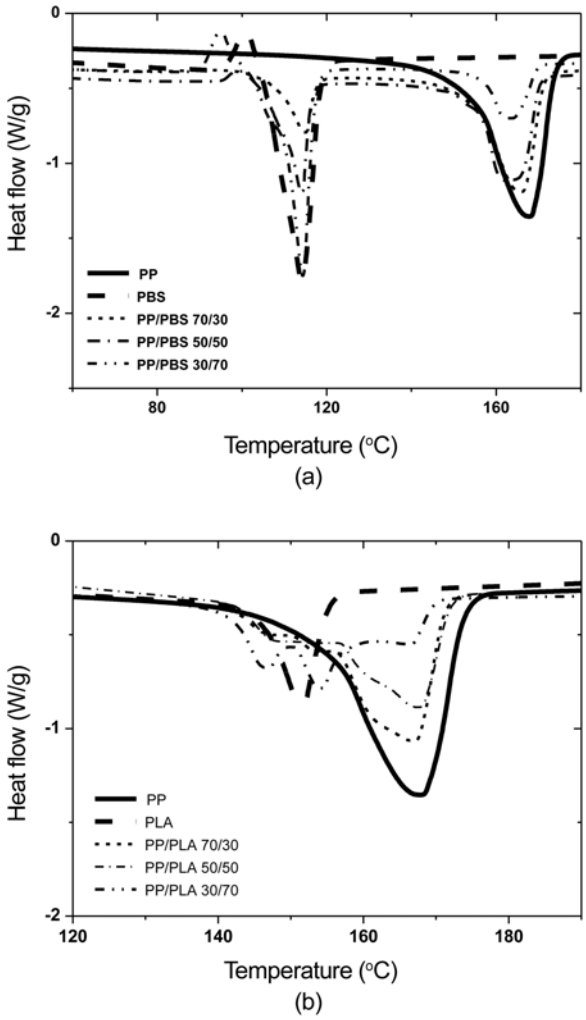

Figure 5. DSC heating curves of (a) PP/PBS and (b) PP/PLA blends as a function of composition.

Table 3. DSC results of PP/PBS and PP/PLA blends as a function of composition

PP/PBS	100/0	70/30	50/50	30/70	0/100
T_m, PP (°C)	167.8	166.1	163.2	163.7	-
T_m, PBS (°C)	-	114.7	114.0	114.4	114.0
T_g, PP (°C)	-2.6	-2.4	-3.1	-2.6	-
T_g, PBS (°C)	-	-18.1	-15.7	-16.4	-17
PP/PLA	100/0	70/30	50/50	30/70	0/100
T_m, PP (°C)	167.8	167.2	167.9	154.6	-
T_m, PLA (°C)	-	146.3	147.6	146.2	151.3
T_g, PP (°C)	-2.6	-2.5	-2.7	-2.7	-
T_g, PLA (°C)	-	60.98	61.3	58.5	65.9

systems were immiscible blends. To enhance the interfacial adhesion and mechanical properties of the immiscible blends

of two different polymers, the use of compatibilizers, copolymerization reaction, and interchange reaction of immiscible blends have been extensively studied [9,20].

Dynamic Mechanical Analysis (DMA)

The storage modulus (E') measurements of polymers and polymer blends determine their relevant stiffness, while tan δ measurements give practical information on T_g [17,18]. Figures 6(a) and 6(b) show the temperature dependence of the dynamic storage modulus for PP/PBS and PP/PLA blends as a function of composition. With increasing temperature, the E' values of the PP/PBS and PP/PLA blends significantly decreased due to the increased viscosity and polymer chain mobility of the pure polymer and their blends at higher temperatures [21]. PBS has a higher E' than that of PP below −30 °C and PP has a higher E' than that of PLA below about 0 °C. However, the E' value of PLA significantly decreased at about 60 °C. These results were related with T_g of pure PP, PBS and PLA. With increasing PBS content the PP, the E' value of the PP/PBS blends decreased. This result was confirmed by the decreasing tensile strength of the PP/PBS blends with increasing PBS content. The decreased E' value of the PP/PBS blends may have been caused by the low compatibility and immiscible blends of the binary PP/PBS blends. However, below about 20 °C, the E' value of the PP/PLA blends increased with increasing PLA content in the PP, confirming the higher E' value of pure PP than that of PLA.

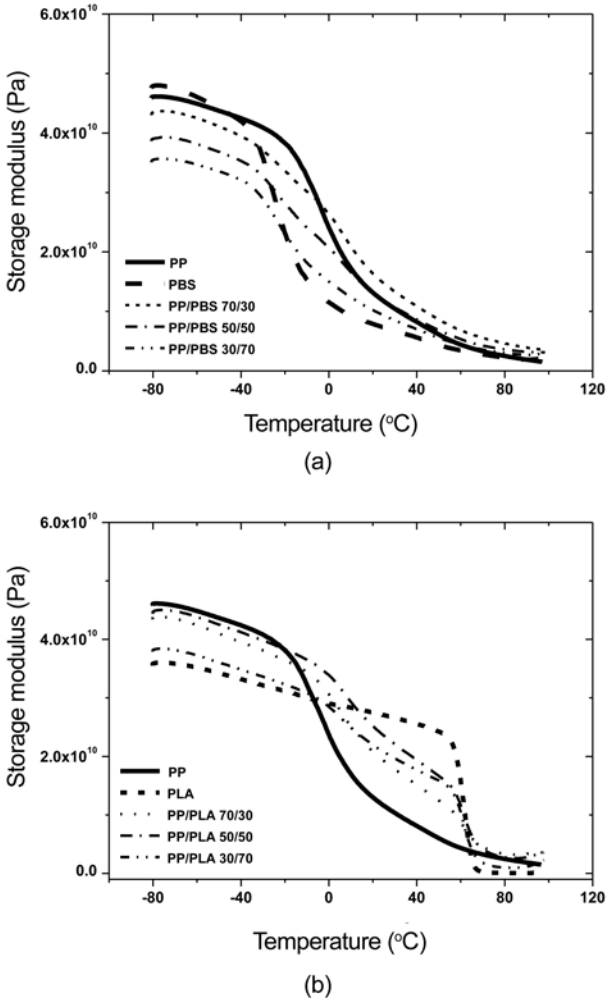

Figure 6. Temperature dependence of the dynamic storage modulus for (a) PP/PBS and (b) PP/PLA blends as a function of composition.

In general, the most popular method to determine the miscibility of a blend system is by plotting the composition dependency of T_g. The temperature dependence of tan δ for the PP/PBS and PP/PLA blends is presented in Figure 7. Tan δ was obtained from the ratio of E' (elastic phase) and E'' (viscous phase). The tan δ_{max} peak can also provide information on the T_g and energy dissipation of the polymer [21,22]. With increasing temperature, the tan δ values of the PP/PBS blends increased due to the increased polymer chain mobility of their blends. Table 4 summarizes the T_g calculated from the maximum of the tan δ peak for the PP/PBS and PP/PLA blends. The T_g of pure PP, PBS and PLA was 4.1 °C, −17.9 °C and 68.4 °C, respectively. However, the PP/PBS and PP/PLA blends showed two distinct T_g values in Table 4. Also, the $T_{g,PP}$ of the PP/PBS and PP/PLA blends slightly decreased with increasing PBS and PLA content. These results indicated that PP has a low compatibility with PBS and PLA and that the PP/PBS and PP/PLA blends were completely immiscible, polymer blend systems. A single T_g value for a

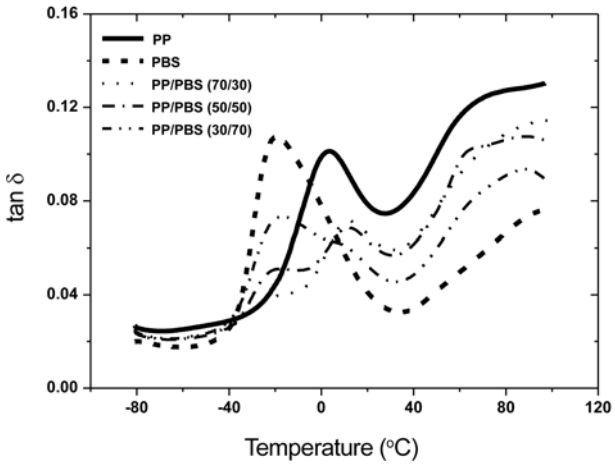

Figure 7. Temperature dependence of tan δ of PP/PBS blends as a function of composition.

Table 4. Tan Δ_{max} peak temperature for PP/PBS and PP/PLA blends

PP/PBS	100/0	70/30	50/50	30/70	0/100
T_g, PP (°C)	4.1	12.1	11.9	9.1	-
T_g, PBS (°C)	-	-21.2	-17.7	-16.6	-17.9
PP/PLA	100/0	70/30	50/50	30/70	0/100
T_g, PP (°C)	4.1	11.2	11.5	9.6	-
T_g, PLA (°C)	-	65.9	65.1	66.3	68.4

twin-polymer blend system indicates a miscible system [18].

Morphological Observation

Figure 8 shows SEM micrographs of the fracture surface of the tensile specimens of the PP/PBS and PP/PLA blends. The volume ratio of the blending components is known to play a predominant role in determining which of the two blending components forms the disperse phase and which the matrix phase [20]. From Figure 8 in the 70/30 PP/PBS and PP/PLA blends, it could be seen that PP acted as the continuous phase, while PBS and PLA served as the dispersed phase because the PP content was larger than that of PBS and PLA. In these figures, the PP and PLA domains have well defined spherical shape and very broad size distribution, which is a typical morphology of immiscible polymer blends. The immiscibility of the PP/PBS and PP/PLA blends resulted in phase segregation and poor dispersion [23,24]. Furthermore, the presence of many holes in the SEM micrographs of the 50/50 PP/PBS and PP/PLA blends indicated the retreat of particles and hence the lack of any adhesion between the phases. The morphological analysis of the present study clearly demonstrated the immiscibility of the PP/PBS and PP/PLA blends. Without special treatment of a direct mixture of the PP/PBS and PP/PLA blends, these blends lead to incompatible blends and poor mechanical properties.

Bio-composites Measurement

Mechanical Properties

Figures 9 and 10 show the tensile and flexural strengths of the BF- and WF-filled, (a) PP/PBS and (b) PP/PLA blend bio-composites as a function of composition. In the incorporation of BF and WF in the PP/PBS and PP/PLA blends, the tensile strength of these bio-composites decreased compared to the tensile strength of the PP/PBS and PP/PLA blends. A similar result was expected for the flexural strength of BF and WF in the PP/PBS and PP/PLA bio-composites. At the PP/PBS and PP/PLA blend ratio of 70/30, the tensile strength of the BF- and WF-filled, PP/PBS and PP/PLA bio-composites was similar to the tensile and flexural strengths of the BF- and WF-filled, PP and PBS bio-composites [2,25]. These results suggested that natural-flour-filled PP/PBS and PP/PLA bio-composites are an acceptable substitute for natural-flour-filled non-biodegradable plastic composites to enhance their biodegradability and reduce manufacturing costs. The decreased tensile and flexural strengths of these bio-composites were due to the weak interfacial adhesion and low compatibility between the hydrophilic natural flour and hydrophobic matrix.

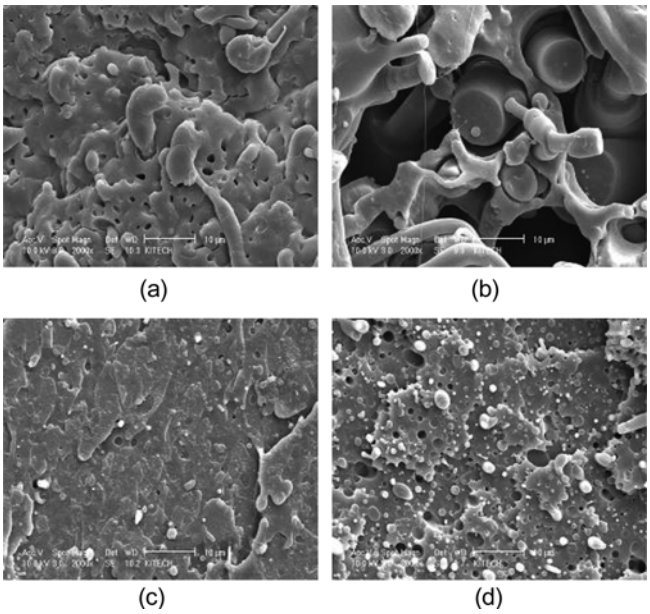

Figure 8. SEM micrographs (2000×) of the fracture surface of tensile specimens of (a) PP/PBS:70/30, (d) PP/PBS:50/50, (c) PP/PLA:70/30 and (d) PP/PLA:50/50 of PP/PBS and PP/PLA blends as a function of composition.

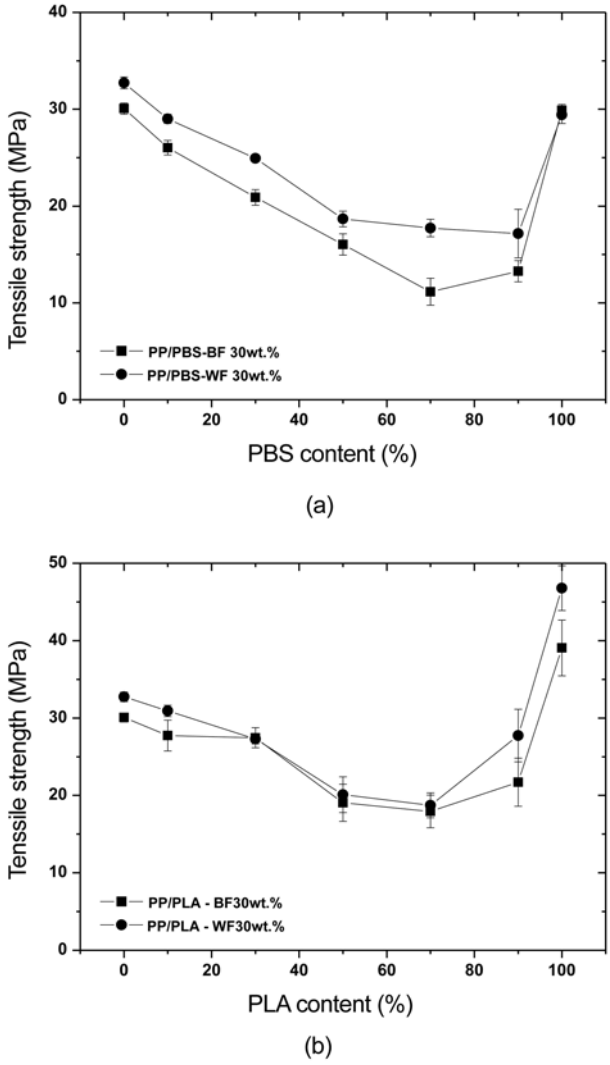

Figure 9. Tensile strength of BF- and WF-filled, (a) PP/PBS and (b) PP/PLA bio-composites as a function of composition.

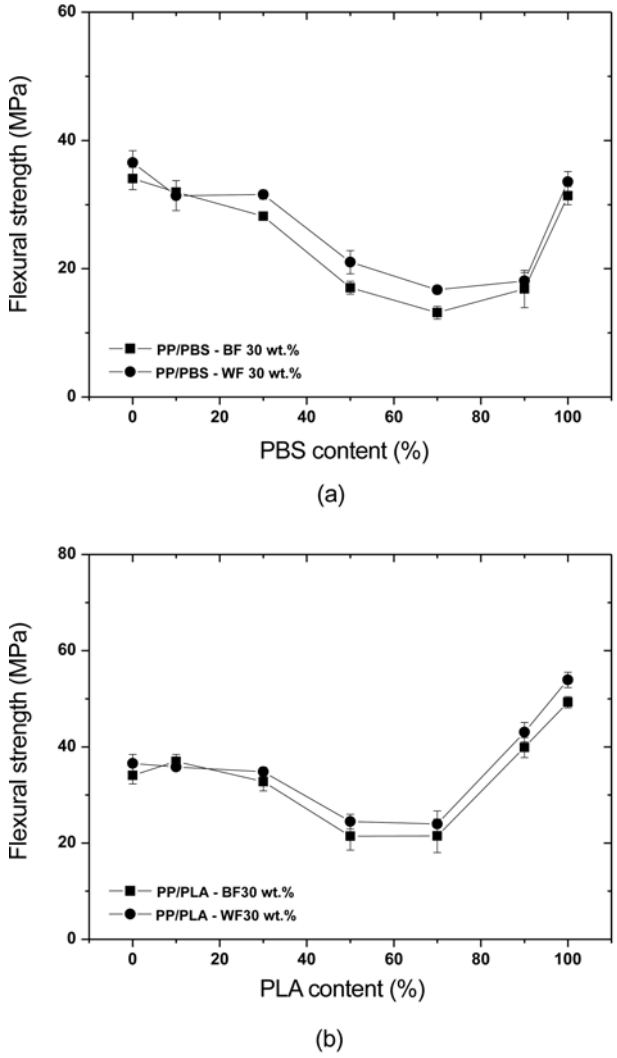

Figure 10. Flexural strength of BF- and WF-filled, (a) PP/PBS and (b) PP/PLA bio-composites as function of composition.

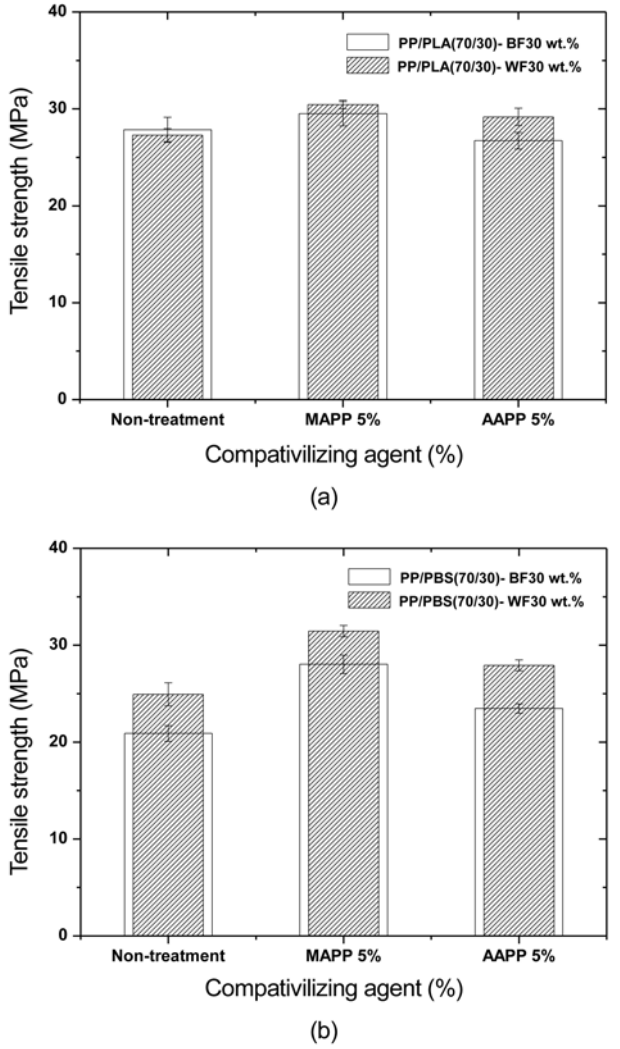

Figure 11. Tensile strength of BF- and WF-filled, (a) PP/PBS: 70/30 and (b) PP/PLA: 70/30 bio-composites as a function of compatibilizing agent type.

BF and WF contain the hydroxyl groups of cellulose and hemicellulose ingredients which reduce the interfacial adhesion wetting at the interface [25,26]. The main disadvantage encountered during the incorporation of natural flour into polymers is the lack of good interfacial adhesion between the two components, which results in poor properties of the final materials [27]. In addition, the tensile and flexural strengths of the WF-filled PP/PBS and PP/PLA bio-composites were slightly higher than those of the BF-filled PP/PBS and PP/PLA bio-composites, due to the smaller particle size of WF, which leads WF to form smaller agglomerates than the bigger particle size of BF in the matrix [26]. In this study, MAPP and AAPP were used as compatibilizing agents to increase the interfacial adhesion and mechanical properties of the BF- and WF-filled, PP/PBS and PP/PLA bio-composites. Figures 11 and 12 show the tensile and flexural strengths of the BF- and WF-filled, (a) PP/PBS and (b) PP/PLA blend bio-composites according to the compatibilizing agent types. The tensile and flexural strengths of the MAPP- and AAPP-treated, BF- and WF-filled, PP/PBS and PP/PLA blend bio-composites were higher than those of the non-treated bio-composites. MAPP underwent esterification reaction or hydrogen bonding at the interface between the hydroxyl groups of the BF and WF on one side and the carboxylic groups of the MAPP diffused matrix polymer on the other side [26]. Also, BF and WF was fully supplied with hydroxyl groups and that in this reaction the -CH_2OH and -COOH groups were converted to ester groups [28]. The tensile and flexural strengths of MAPP-treated, BF- and WF-filled, PP/PBS and PP/PLA bio-composites were higher than those of the AAPP-treated bio-composites, indicating that the anhydride functional group of MAPP reacts easily with the OH groups of BF and WF. Therefore, the bio-composites with 5% MAPP content had the highest mechanical properties

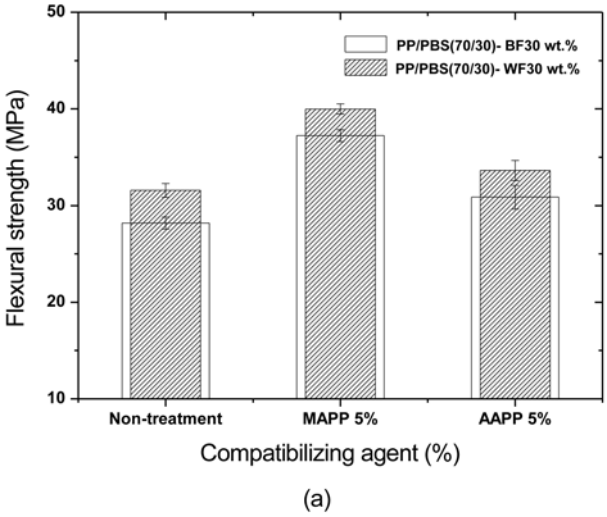

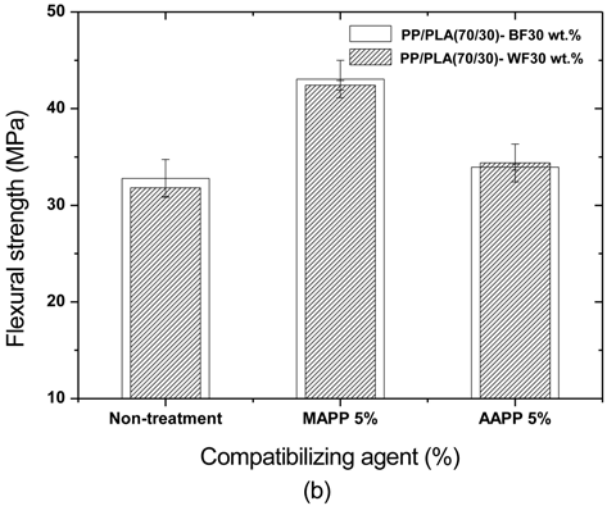

Figure 12. Flexural strength of BF- and WF-filled, (a) PP/PBS: 70/30 and (b) PP/PLA:70/30 bio-composites as a function of compatibilizing agent type.

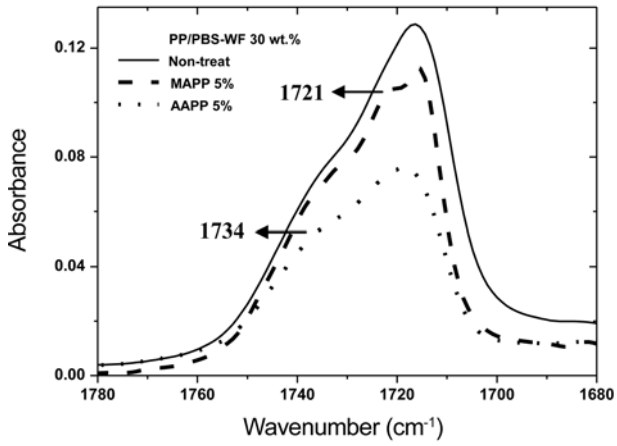

Figure 13. FTIR-ATR spectra of MAPP- and AAPP-treated and non-treated, WF-filled PP/PBS (70/30) blend bio-composites.

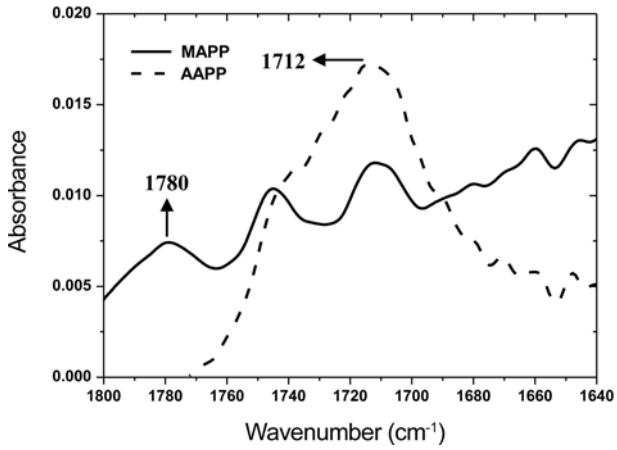

Figure 14. FTIR-ATR spectra of MAPP and AAPP.

and this content was therefore chosen as the proper addition rate to improve the interfacial adhesion and mechanical properties of the bio-composites.

Attenuated Total Reflectance (FTIR-ATR) Spectroscopy

FTIR-ATR spectra of the MAPP- and AAPP-treated and non-treated, WF-filled, PP/PBS (70/30) bio-composites are shown in Figure 13. This figure clearly shows the two special peaks that are evident at 1721 cm^{-1} and 1734 cm^{-1}, while Figure 14 shows two absorption peaks at 1780 $cm^{-1}$and 1712 cm^{-1}. These peaks were assigned to symmetric C=O stretching (1780 cm^{-1}) of MA functional groups of MAPP and C=O stretching (1712 cm^{-1}) of AA functional groups of AAPP, respectively [26,28]. This MAPP peak indicated that the bands at 1721 cm^{-1} were due to the stretching vibration of the ester carbonyl groups (C=O) of the MAPP-treated, WF-filled PP/PBS (70/30) bio-composites. This result suggested that MAPP interacts with WF by forming covalent linkage and ester bonding between the MA group of MAPP and the hydroxyl groups at the WF [26,29]. From this AAPP peak, the absorption peak at 1734 cm^{-1} was attributed to the ester carbonyl group of the AAPP-treated, WF-filled, PP/PBS (70/30) bio-composites. This result indicated that the AA group of AAPP has carboxyl groups to react with the hydroxyl groups of WF as a result of converting the ester group [28]. Similar results were expected with the MAPP- and AAPP-treated, BF- and WF-filled, PP/PLA (70/30) bio-composites.

Morphological Observation

Figure 15 shows SEM micrographs of the tensile fracture surface of the (a) non-treated and (b) MAPP-treated, BF- and WF-filled, PP/PBS (70/30) bio-composites. This figure shows that BF and WF were removed completely from the matrix and that bigger gaps appeared between the BF and WF and the matrix in the tensile fracture surface, which is evidence of weak interfacial adhesion at the interface. Weak

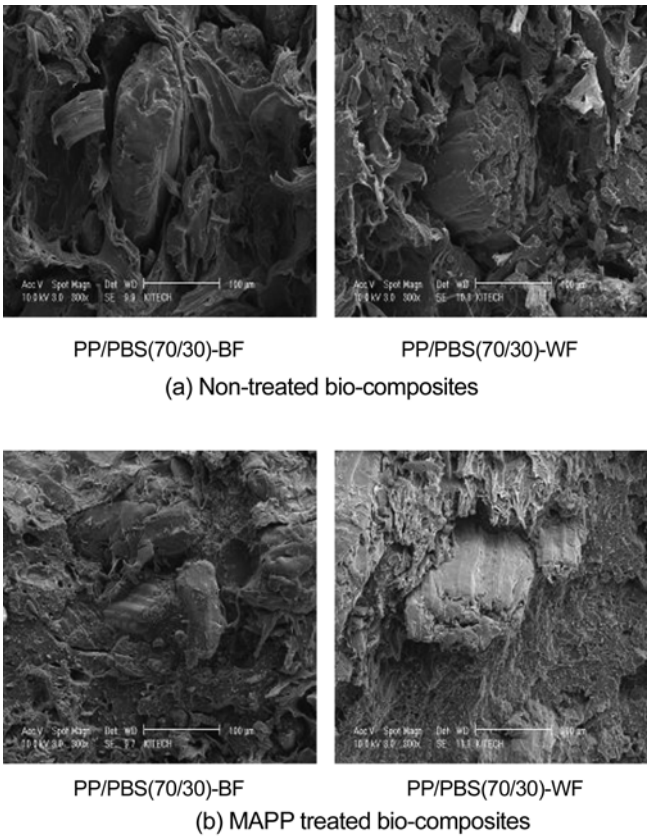

Figure 15. SEM micrographs of the tensile fracture surface of (a) non-treated and (b) MAPP-treated, BF- and WF-filled, PP/PBS (70/30) bio-composites (300×).

interfacial adhesion easily led to complete debonding from the matrix in the tensile fracture surface [26]. The SEM micrographs of the MAPP-treated, BF- and WF-filled, PP/PBS (70/30) bio-composites were also presented in Figure 15. This figure show the good bonding of BF and WF into the matrix and the paucity of pulled-out traces from the matrix, thereby indicating the better dispersion, wetting and interfacial adhesion of the MAPP-treated, BF- and WF-filled, PP/PBS (70/30) bio-composites [25]. These results were confirmed by the increasing tensile and flexural strengths of the MAPP-treated, BF- and WF-filled, PP/PBS (70/30) bio-composites.

Conclusion

The tensile strength of the PP/PBS blends decreased with increasing PBS content. However, the tensile strength of the PP/PLA blends increased with increasing PLA content due to the higher tensile strength of PLA compared to PP. The thermal stability of the PP/PBS and PP/PLA blends decreased with increasing PBS and PLA content. The T_m and T_g of pure PP, PBS and PLA showed a single peak but DSC results presented two peaks for the T_m and T_g of the PP/PBS and PP/PLA blends. With increasing PBS content in the PP, the E' value of the PP/PBS blends decreased however, below about 20 °C, the E' value of the PP/PLA blends increased with increasing PLA content due to the higher E' value of pure PP than that of PLA. The tan δ_{max} peak temperature (T_g) of the PP/PBS and PP/PLA blends showed two distinct T_g values, indicated the immiscibility of the PP/PBS and PP/PLA polymer blend systems. These results were also confirmed by the SEM micrographs of the 50/50 PP/PBS and PP/PLA blends, in which the presence of many holes evidenced the retreat of particles and thus the lack of any adhesion between the phases. At the blend ratio 70/30 of PP/PBS and PP/PLA, the tensile and flexural strengths of the BF- and WF-filled, PP/PBS and PP/PLA blend bio-composites were similar to those of the BF- and WF-filled, PP and PBS bio-composites. The mechanical properties of the MAPP- and AAPP-treated, BF- and WF-filled, PP/PBS and PP/PLA blend bio-composites were higher than those of the non-treated bio-composites. This result was confirmed by the presence of pulled-out traces on the SEM micrographs of the tensile fracture surface between the natural flour and matrix and by the FTIR-ATR spectral results for the stretching vibration of the ester carbonyl groups (C=O) of the WF-filled, PP/PBS (70/30) bio-composites at 1721 cm^{-1} (MAPP) and 1739 cm^{-1} (AAPP). These study results confirmed the suitability of natural-flour-filled, PP/PBS and PP/PLA blend bio-composites to act as substitutes for natural-flour-filled, non-biodegradable plastic composites for the purpose of enhancing the biodegradability and reducing the manufacturing cost of natural-flour-filled, biodegradable plastics.

References

1. J. H. Zhao, X. Q. Wang, J. Zeng, G. Yang, F. H. Shi, and Q. Yan, *J. Appl. Polym. Sci.*, **97**, 2273 (2005).
2. H.-S. Kim, H.-J. Kim, J.-W. Lee, and I.-G. Choi, *Polym. Degrad. Stabil.*, **91**, 1117 (2006).
3. J. Li, Y. He, and Y. Inoue, *Polym. Int.*, **23**, 949 (2003).
4. M. Shibata, S. Oyamada, S. Kobayashi, and D. Yaginuma, *J. Appl. Polym. Sci.*, **92**, 3857 (2004).
5. M. S. Huda, L. T. Drzal, A. K. Mohanty, and M. Misra, *Compos. Sci. Technol.*, **66**, 1813 (2006).
6. D. S. Rosa, C. G. F. Guedes, and M. A. G. Bardi, *Polym. Test.*, **26**, 209 (2007).
7. J. Kim, J. H. Kim, T. K. Shin, H. J. Choi, and M. S. Jhon, *Eur. Polym. J.*, **37**, 2131 (2001).
8. Y. J. Kim and O. O. Park, *J. Environ. Polym. Degrad.*, **7**, 53 (1999).
9. J. John, R. Mani, and M. Bhattacharya, *J. Polym. Sci., Part A: Polym. Chem.*, **40**, 2003 (2002).
10. H. Pehlivan, D. Balkose, S. Ulku, and F. Tihminlioglu, *J. Appl. Polym. Sci.*, **99**, 143 (2006).
11. E. D. Ray, P. R. Gruber, and D. E. Henton, *Adv. Mater.*, **23**, 1841 (2000).
12. L. Jiang, M. P. Wolcott, and J. Zhang, *Biomacromolecules*, **7**, 199 (2006).

13. Y. F. Shih, T. Y. Wang, R. J. Jeng, J. Y. Wu, and C. C. Teng, *J. Polym. Environ.*, **15**, 151 (2007).
14. Y. Ichikawa, "Asia's First Bioplastic Conference and Exhibition", 49 (2006).
15. Y. Kori, K. Kitagawa, and H. Hamada, *J. Appl. Polym. Sci*., **98**, 603 (2005).
16. H. Ismail and M. Nasir, *Polym.Test*., **21**, 163 (2002).
17. H.-S. Kim, H.-S. Yang, H.-J. Kim, B.-J. Lee, and T.-S. Hwang, *J. Therm. Anal. Cal*., **81**, 299 (2005).
18. P. S. George, Oxford University Press, 22 (2003).
19. S. Kim and H.-J. Kim, *Macromol. Mater. Eng*., **29**, 339 (2007).
20. R. Qi, J. Nie, C. Zhou, D. Mao, and B. Zhang, *J. Appl. Polym*. *Sci*., **102**, 6081 (2006).
21. H.-S. Kim, S. Kim, H.-J. Kim, and H.-S. Yang, *Thermochim. Acta*., **451**, 181 (2006).
22. M. Shibata, N. Teramoto, and Y. Inoue, *Polym*., **48**, 2257 (2007).
23. A. Tedesco, R. V. Barbosa, S. M. B. Nachtigall, and R. S. Mauler, *Polym. Test*., **21**, 11 (2002).
24. Y. F. Kim, C. N. Choi, Y. D. Kim, K. Y. Lee, and M. S. Lee, *Fiber. Polym*., **5**, 270 (2004).
25. H.-S. Kim, S. Kim, and H.-J. Kim, *Macromol. Mater. Eng*., **291**, 762 (2006).
26. H.-S. Kim, B.-H. Lee, S.-W. Choi, S. Kim, and H.-J. Kim, *Compos. Part A*., **38**, 1473 (2007).
27. V. Tserki, P. Matzinos, and C. Panayiotou, *Compos. Part-A*., **37**, 1231 (2006).
28. C. S. Wu, *Macromol. Biosci*., **5**, 352 (2005).
29. F. Marti-Ferrer, F. Vilaplana, A. Ribes-Greus, A. Benedito-Borras, and C. Sanz-Box, *J. Appl. Polym. Sci*., **99**, 1823 (2005).